Astron. Astrophys. 65, 273—277 (1978)

ASTRONOMY AND ASTROPHYSICS

Acoustic Waves in the Solar Atmosphere

IV. On the Efficiency of One-dimensional Hydrodynamic Codes

R. Hammer and P. Ulmschneider

Institut für Astronomie und Astrophysik der Universität Würzburg, Am Hubland, D-8700 Würzburg, Federal Republic of Germany

Received August 8, 1977

Summary. In this fourth paper of a series on acoustic waves in stellar atmospheres the leapfrog type finite difference method and various forms of modified characteristics methods are compared for accuracy and efficiency. Although the choice of the method depends somewhat on the application we found that the most accurate and the most efficient method is a modified characteristics method with natural cubic spline interpolation.

Key words: acoustic waves — hydrodynamics

1. Introduction

In recent years a growing number of hydrodynamic calculations has been made to investigate acoustic wave processes in the solar and in stellar atmospheres. Various mathematical methods are used for this purpose.

The explicit second order leapfrog type finite difference method (FDM) using pseudoviscosity (Von Neumann and Richtmyer, 1950) was employed for instance by Christy (1964), Leibacher (1971), Stein and Schwartz (1972, 1973), Klein et al. (1976). The modified characteristics method (MCM) with fixed time steps (Hartree, 1952; Lister, 1960; Hoskin, 1964) on the other hand was used by Stefanik (1973), Chow (1973), Ulmschneider et al. (1977a, Paper I of this series), Kalkofen and Ulmschneider (1977, Paper II), Ulmschneider and Kalkofen (1977, Paper III), Ulmschneider et al. (1977b). Because these computations, especially with the inclusion of radiation, ionization, statistical equilibrium etc., are highly time consuming on the computer and yet of fundamental importance for the understanding of the chromosphere, transition layer and corona, a detailed comparison singling out the most accurate and efficient method is of great urgency. It is the aim of this fourth in a series of papers on acoustic waves to make such a comparison as far as is presently possible.

Send offprint requests to: R. Hammer

For this purpose the exact simple wave solution of a sinusoidally oscillating piston is employed. Comparisons are also made for the constantly accelerated piston and for a sinusoidal piston in a gravitational atmosphere. A short discussion on the different radiation treatments is given but a detailed comparison is beyond the scope of this work.

2. The Hydrodynamic Codes

The MCM computes the solution at a given point P by backtracing the characteristics at this point to their intersection points with the former time level, where the solutions are determined by interpolation. The characteristic equations then give the solution at P. Since this solution influences the slope of the characteristics, the whole process has to be iterated until convergence is reached. The type of interpolation at the lower time level is of great importance for the success of the method. We used three different types of interpolation,

MCMP : interpolation by quadratic parabolas,

MCMA : interpolation by weighted quadratic parabolas as used by Kurucz (1970, p. 16),

MCMS : interpolation by natural cubic spline functions.

For the details of the MCM see Papers I and II of this series as well as Ulmschneider et al. (1977b).

The interpolation accuracy at grid point i is influenced by the Courant number,

$$L_i = c_i \frac{\Delta t}{\Delta x_i} = \frac{\rho_i}{\rho_i(t=0)} c_i \frac{\Delta t}{\Delta a_i}. \quad (1)$$

This quantity determines the spatial distance between the grid points and the intersection points of the characteristics with the lower time level. Here, c denotes the sound velocity, ρ the density, and x and a the Eulerian and Lagrangian coordinates respectively.

The overshooting of the interpolation curve which may appear with methods MCMP and MCMS is avoided in MCMA by weighting the coefficients of the backward parabola $y_i(a)$ and of the forward parabola

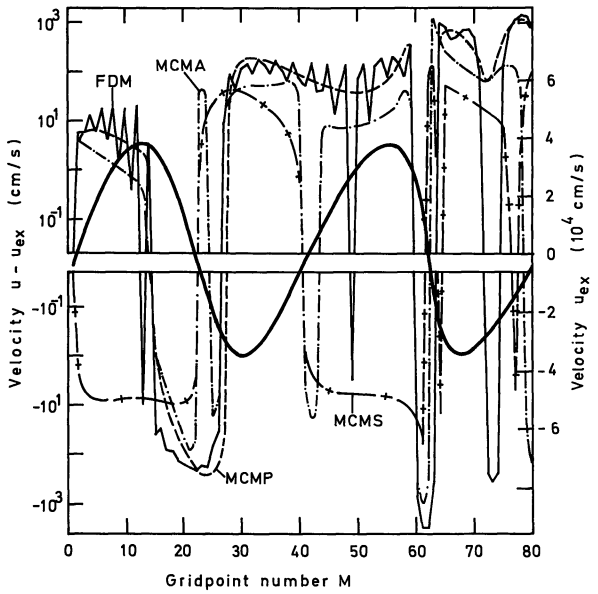

Fig. 1. The exact velocity profile u_{ex} (drawn heavy) as function of Lagrangian height represented by an equidistant grid. Also shown is the deviation of the velocity from u_{ex} for the four numerical methods indicated

$y_{i+1}(a)$ inversely by the second derivatives of these curves, so that

$$y(a)=wy_i(a)+(1-w)y_{i+1}(a) \tag{2}$$

with

$$w=\frac{|y''_{i+1}|}{|y''_i|+|y''_{i+1}|}$$

is used as interpolation curve in the range $a_i \leqq x \leqq a_{i+1}$.

In the FDM a pseudoviscosity term,

$$q=\begin{cases}(c_q\,\Delta a)^2\left(\dfrac{\partial u}{\partial a}\right)^2\rho & \text{if } \dfrac{\partial u}{\partial a}<0\\ 0 & \text{if } \dfrac{\partial u}{\partial a}\geqq 0\end{cases} \tag{3}$$

is added to the pressure in the momentum and energy equations. Here, u is the gas velocity, and c_q is a free parameter. Although q originally had been introduced to avoid discontinuities and to account for shock heating, its inclusion also improves the accuracy in the case of continuous flows. This is due to the fact that artificial viscosity does smooth the oscillations inherent in the FDM scheme which are seen e.g. in Figure 1. As is shown in Section 3 below, a certain value of c_q will minimize the errors experienced in the FDM method.

We coded the MCM and FDM schemes for the computation of waves in a one-dimensional, compressible, nonisothermal gas under the action of a constant gravitational acceleration g. In order to compare our numerical results with analytic solutions we assume first the medium to be isothermal with $g=0$ and at rest at time $t=0$. The waves were induced by a piston at the left boundary of the medium (at grid point 1), moving sinusoidally with period τ such that at time t

$$u(t)=M_0\,c_0\sin\left(\frac{2\pi}{\tau}t\right), \tag{4}$$

where c_0 is the sound velocity at $t=0$ and M_0 the Mach number. With these special initial and boundary values, the waves are simple waves (Courant and Friedrichs, 1948, pp. 59, 60, 92–95) with the C^+-characteristics being straight lines, and the analytical solution at any point of the (a,t)-plane may be computed using the constancy of the Riemann invariants (Courant and Friedrichs, 1948, pp. 87, 88) along the characteristics.

The shock insertion point (a_s, t_s) is defined by the earliest intersection point of two characteristics of the same kind. There the solution is no longer unique. Therefore, this point may be computed as the cusp of the envelope of the characteristics (Courant and Friedrichs, 1948, pp. 107–115). For a piston motion after Equation (4), this gives

$$t_s=\begin{cases}t_K+\dfrac{\tau}{(\gamma+1)\pi}\left(\dfrac{\gamma(\gamma+1)}{(1+2\,\gamma\,(\gamma+1)\,M_0^2)^{1/2}-1}\right. & \\ \left.-\dfrac{\gamma(\gamma-1)}{2}\right)^{1/2} & \text{for } M_0<0\\ \dfrac{\tau}{(\gamma+1)\,\pi\,M_0} & \text{for } M_0>0\end{cases} \tag{5}$$

and

$$a_s=c_0(t_s-t_K)\left[1+\frac{\gamma-1}{2}M_0\sin\left(\frac{2\pi}{\tau}t_K\right)\right]^{\frac{\gamma+1}{\gamma-1}}. \tag{6}$$

Here, γ denotes the ratio of specific heats and t_K is the time at which the C^+-characteristic through the shock point originates at the piston:

$$t_K=\begin{cases}\dfrac{\tau}{2\pi}\left[\pi-\arcsin\left(\dfrac{1-(1+2\,\gamma\,(\gamma+1)\,M_0^2)^{1/2}}{(\gamma+1)\,M_0}\right)\right] & \\ \text{for } M_0<0 & \\ 0 \quad \text{for } M_0>0.\end{cases} \tag{7}$$

3. Accuracy

Under solar chromospheric conditions ($\gamma=5/3$, $c=7.3$ E 5 cm/s), Equation (5) gives a shock time of 86.4 s for a wave of period $\tau=30$ s and amplitude $M_0=-0.05$. Figure 1 shows the exact velocity profile $u_{ex}(a)$ of the wave as function of Lagrange height a at the time 60.75 s. Also shown in Figure 1 are the deviations $u-u_{ex}$ of the numerical result for all four methods. For these computations, we used an equidistant spatial mesh with grid point density $n=40$ grid points per wavelength. The total number of gridpoints was $N=80$. The boundary condition on the right was chosen to transmit forward-facing simple waves without reflection (see Paper I).

The errors of the MCMS method are roughly proportional to the second derivative of the exact curve.

This may be due to the tendency of spline interpolation to underestimate the curvature. The deviations of the other three methods have mostly the same sign as the slope of the exact solution, with the exception of the peaks which occur in the MCMA near turning-points of u_{ex}. For all methods, the largest errors occur in the region of high compression (i.e. with steeply descending velocity profile) near grid point 62, which is soon going to steepen into a shock near point 96.

A simple parameter which allows to judge the accuracy may be defined in various ways. Two commonly used choices are the maximum norm of the error vector, $\max |u_i - u_{i,ex}|$, or the Euclidean norm. In a scaled and dimensionless form, the Euclidean norm may be written

$$F(M)=\left(\sum_{i=1}^{M}(u_i-u_{i,ex})^2\right)^{1/2}\Big/\left(\sum_{i=1}^{M}u_{i,ex}^2\right)^{1/2} \tag{8}$$

This quantity gives the mean relative error in the gas velocity for grid points 1 through M where $M \leqq N$ is some intermediate grid point. As M is allowed to vary, different regions of a wave (like compression regions or the vicinity of the right boundary) may be investigated separately.

As is demonstrated in Figure 2, this function shows a plateau-like structure which is caused by the fact that the largest errors occur in compression regions. Figure 2 shows that the accuracy of the MCMP and FDM schemes is almost the same, while the MCMA is much better. Spline interpolation, MCMS, gives even smaller errors, especially in the compression region. This scheme is found to be superior to all other methods.

The accuracy of the FDM depends on the pseudoviscosity parameter, the best choice of which is not known a priori. This has been shown for shock propagation by Colombant and Gardner (1976), and is also true for adiabatic flows. The above calculations have been done with $c_q^2=0.88$, since this value minimizes the height of the lower plateau. For larger values of c_q^2, the errors due to irreversible viscous heating increase, while for smaller values the oscillations of the $u-u_{ex}$ curve increase. For example in computations with $c_q^2=0$ or $c_q^2=1.7$, the errors are increased by about 10% relative to the optimum case with $c_q^2=0.88$. The optimum viscosity parameter depends on the definition of the accuracy as well as on the shape of the wave and the grid point density. Our sinusoidal wave, for instance, requires an increasing pseudoviscosity for decreasing grid point density.

4. Computing Time and Efficiency

All codes were written in the same language, namely the ASA standard version of FORTRAN IV. Moreover, similar programming and storage techniques have been used. The net computing times—i.e. the times without data initialisation, input, and output—are therefore a good measure for comparison of the speed of the codes.

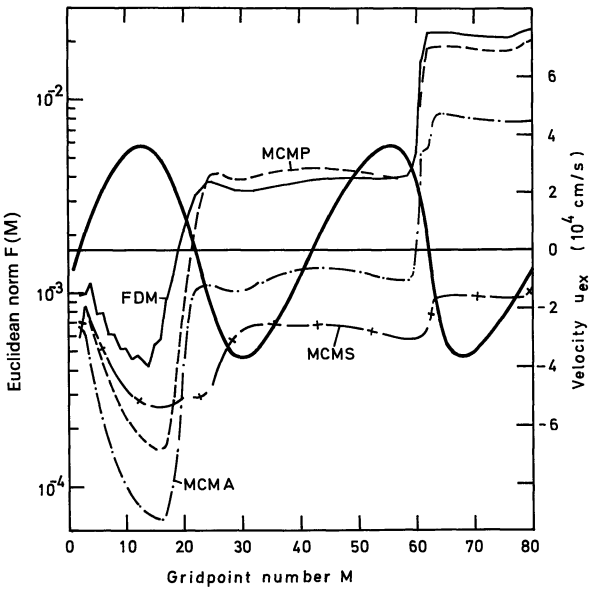

Fig. 2. Cumulative errors measured in the Euclidean norm $F(M)$ as function of grid point number M for the four methods. Also shown is the exact velocity profile u_{ex} (drawn heavy)

Time step and grid point density n are interlocked by stability criteria. These are the Courant-Friedrichs-Lewy condition, $L \leqq 1$, for the MCM schemes, and a somewhat stronger condition in the case of the FDM which has to be tested experimentally (Richtmyer and Morton 1967, p. 329). Therefore, one would expect that

$$\text{computing time} \sim (\Delta a)^{-2} \sim n^2 \tag{9}$$

holds. We found that this relation is fulfilled quite accurately by all codes.

However, the relative computing times of the four methods differ: While the MCMP and FDM need almost the same time, the MCMA and MCMS codes are slower by about 35 and 55%, respectively. Since FDM and MCM schemes use different stability criteria, these numbers are slightly different when using other amplitudes and different types of waves. We tested such cases with the MCMP and FDM codes, and found that the above result is representative.

Since all codes are based on second order methods, the errors should be inversely proportional to the square of the grid point density n,

$$F(N) \sim n^{-2} \tag{10}$$

As is shown in Figure 3, this relation holds quite well in the limit $n \to \infty$.

Neither computing time nor accuracy alone are good parameters for the judgement of the quality of a code. However, since computing time is proportional to n^2 [Eq. (9)] and the errors are roughly proportional to n^{-2} [Eq. (10)], the quantity

$$\eta = (\text{error} \cdot \text{computing time})^{-1} \tag{11}$$

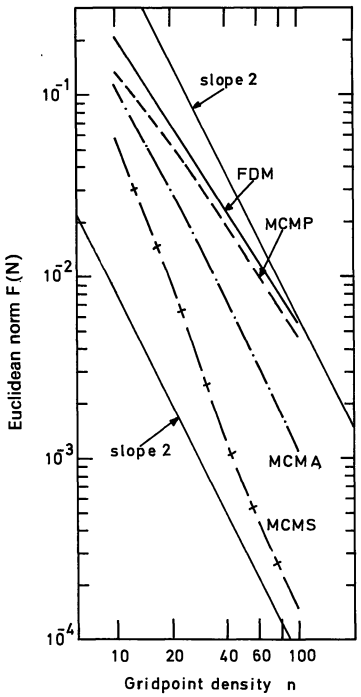

Fig. 3. Cumulative errors measured in the Euclidean norm $F(N)$ as function of the grid point density per wavelength n

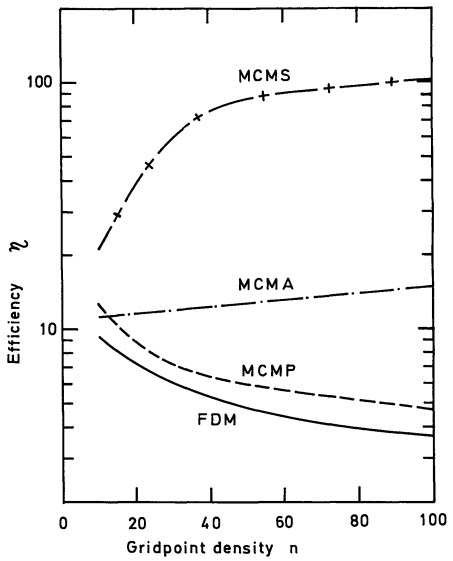

Fig. 4. Efficiency η, the inverse of the product error times computing time, as function of the grid point density per wavelength n

should be nearly a constant for each code, at least in the limit $n\to\infty$. We therefore use η as a measure for the efficiency of a code. Figure 4 shows, for all codes, that η varies only slightly with grid point density. The error has been measured by $F(N)$, but the qualitative results are the same if the maximum norm or any other value of $F(M)$ is used instead of $F(N)$.

Figure 4 demonstrates clearly that the MCMP code is only marginally (by about 20%) more effective than the FDM scheme. Interpolation by weighted parabolas yields a significant improvement. The most effective code, however, is MCMS. For not too small values of n, it is superior to the other methods by an order of magnitude. For small grid point densities, the differences between the curves decrease.

5. Constantly Accelerated Piston, Gravitational Atmosphere

In addition to the sinusoidal piston we have compared the different codes for the constantly accelerated piston. Here exact analytic solutions are known (Landau and Lifshitz 1959, p. 370). The results were found to be similar to what we found for the sinusoidal piston and are thus not repeated here.

For the more interesting case of a sinusoidal piston with gravity no exact solutions can be constructed. Here one has to rely on the property that for zero step size ($n\to\infty$) the exact solution is approached. We found that for this nonisentropic case the overall results described for the sinusoidal, $g=0$ case still apply. In the most severe nonisentropic cases with large temperature gradients (see also Ulmschneider et al., 1977b) the spline interpolation may tend to show oscillations at the trailing edge of the velocity profile near shock formation. These oscillations have even greater amplitudes in the MCMP but do not occur in the MCMA scheme due to the higher intrinsic dissipation of this interpolation method. In the FDM scheme such oscillations are likewise found and may even appear in isentropic cases. Here increasing c_q will suppress the oscillations. Since as shown in Figures 1 and 2 the most severe errors occur in the compression region these oscillations do not greatly affect the total accuracy. They may however present a problem for the numerical procedure to find shocks.

6. Non Hydrodynamic Criteria

The codes for the computation of acoustic waves in stellar atmospheres are not judged by the treatment of the hydrodynamics alone but also by the way how they solve the equations of radiative transfer, of the ionization equilibrium and, if non-LTE effects are important, how they solve the statistical equations. In recent computations that include radiation (Cannon, 1974; Klein et al., 1976; Kneer and Nakagawa, 1976, Papers I–III; Ulmschneider et al., 1977b) the largest time is usually spent in these non hydrodynamic parts of the code. It is very difficult and beyond the scope of this paper to give a comprehensive comparison of these non hydrodynamic methods. For instance we found that the integral method of Paper II for the solution of the transfer equation is by about a factor of four times slower than the Feautrier method used by Klein et al. (1976). However, this is offset by the greater accuracy of the integral method. It is important to note that the choice between integral or differential method for the solution of the

transfer equation does not depend on the hydrodynamic method. In both the FDM and MCM schemes either radiation method may be used. For the hydrodynamical schemes the important fact is that the treatment for the simultaneous solution of the energy and transfer equations in the FDM and MCM schemes both involve iterations, the rapid convergence of which depends heavily on good initial estimates. Thus it is difficult to assess whether the Newton-Raphson iteration in the FDM (e.g. Klein et al., 1976) is more efficient or the D iteration in the MCM (Paper II) where incidentally the number of iterations could be shortened considerably by sacrificing accuracy.

7. Conclusions

Disregarding the efficiency of the non hydrodynamic parts of the four numerical methods, a few general statements may be extracted from our results. These are:

Relative to accuracy, computing time, and efficiency, the MCMP and FDM schemes do not differ much. The FDM method has two disadvantages: First, it needs a pseudoviscosity, the optimum amount of which cannot be known in advance. Second, it needs more timesteps, which is of importance if additional, non hydrodynamic processes are included.

The MCMA, and even more distinctly the MCMS scheme, is by a factor of approximately 1/3 for the MCMA and 1/2 for the MCMS slower but much more accurate and efficient.

In addition it should be noted that for problems in which shocks form out of a continuous flow, the schemes based on the method of characteristics are preferable, since in these codes the shock insertion points may be found as intersection points of characteristics. This is more difficult in the FDM scheme because with pseudoviscosity the characteristics do not intersect and without pseudoviscosity oscillations impair the shock finding. Therefore, the MCM scheme is in principle more appropriate for shock finding and shock fitting problems.

As a consequence, the FDM scheme is only then advantageous if shocks exist and shock fitting is not necessary. In all other cases—i.e. if there are no shocks in the medium, or if there are shocks and exact information on these shocks and their insertion points is needed—the MCMA and MCMS schemes are preferable.

References

Cannon, C.J.: 1974, *J. Quant. Spectrosc. Radiat. Transf.* **14**, 761
Chow, T.L.: 1973, *J. Comp. Phys.* **12**, 153
Christy, R.F.: 1964, *Reviews of Modern Physics* **36**, 555
Colombant, D.G., Gardner, J.H.: 1976, *J. Comp. Phys.* **22**, 389
Courant, R., Friedrichs, K.O.: 1948, Supersonic Flow and Shock Waves, Interscience, New York.
Hartree, D.R.: 1952, Los Alamos Report LA-HU-1
Hoskin, N.E.: 1964, *Meth. Comp. Phys.* **3**, 265
Kalkofen, W., Ulmschneider, P.: 1977, *Astron. Astrophys.* **57**, 193
Klein, R.I., Stein, R.F., Kalkofen, W.: 1976, *Astrophys. J.* **205**, 499
Kneer, F., Nakagawa, Y.: 1976, *Astron. Astrophys.* **47**, 65
Kurucz, R.: 1970, SAO *Spec. Report* 309
Landau, L.D., Lifshitz, E.M.: 1959, Fluid Mechanics, Pergamon Press, London
Leibacher, J.W.: 1971, Ph. D. Thesis, Harvard University
Lister, M.: 1960, in *Math. Methods for Digital Computers I*, Ralston, A., Wilf, H. S., eds., Wiley, New York
Richtmyer, R.D., Morton, K.W.: 1967, Difference Methods for Initial-Value Problems, Interscience, New York
Stefanik, R.P.: 1973, Ph. D. Thesis, Harvard University
Stein, R.F., Schwartz, R.A.: 1972, *Astrophys. J.* **177**, 807
Stein, R.F., Schwartz, R.A.: 1973, *Astrophys. J.* **186**, 1083
Ulmschneider, P., Kalkofen, W., Nowak, T., Bohn, U.: 1977a, *Astron. Astrophys.* **54**, 61
Ulmschneider, P., Kalkofen, W.: 1977, *Astron. Astrophys.* **57**, 199
Ulmschneider, P., Schmitz, F., Renzini, A., Cacciari, C., Kalkofen, W., Kurucz, R., 1977b, *Astron. Astrophys.* **61**, 515
Von Neumann, J., Richtmyer, R.D.: 1950, *J. Appl. Phys.* **21**, 232